Energy and Buildings 126 (2016) 170–176

Contents lists available at ScienceDirect

Energy and Buildings

journal homepage: www.elsevier.com/locate/enbuild

Preparation and characterization of high NIR reflective pigments based in ultramarine blue

Estibaliz Aranzabe[a,*], Pedro María Villasante[c], Ricard March[c], María Isabel Arriortua[b,*], Julen Vadillo[a], Aitor Larrañaga[b], Ana Aranzabe[a]

[a] IK4-Tekniker, Surface Chemistry Unit, Calle Iñaki Goenaga, 5, 20600 Eibar, Gipuzkoa, Spain
[b] Universidad del País Vasco (UPV/EHU), Facultad de Ciencia y Tecnología, Barrio Sarriena S/N, 48940 Leioa, Bizkaia, Spain
[c] Nubiola Pigmentos S.L., Vitoria Kalea, 19, 01400 Laudio, Araba, Spain

ARTICLE INFO

Article history:
Received 18 December 2015
Received in revised form 27 April 2016
Accepted 6 May 2016
Available online 13 May 2016

Keywords:
Ultramarine blue
Total solar reflectance
Lightness
Cool coating

ABSTRACT

Buildings are responsible for at least 40% of energy use in most countries. High reflectance outdoor coatings can bring significant energy savings for building applications. In this context, ultramarine blue pigment (UB) has been modified to increase its near infrared reflectance by depositing a reflecting film based on TiO_2 containing different types and concentrations of nanoparticles (alumina, titania and a mixture of them). The developed pigments were characterized by X-ray diffraction (XRD), field emission scanning electron microscopy (FE-SEM) and laser dispersion.

For testing the performance of the modified pigments, they have been dispersed in a conventional waterborne paint at different percentages and characterized by UV–Vis-NIR spectrophotometry (measuring Total Solar Reflectance and CIE L × a × b ×). All the obtained paints increased the TSR in 2.65% when adding nanoparticles but the maximum value was obtained for an addition of 6 wt.% of titania nanoparticles. Higher contents of nanoparticles led to agglomeration reducing the reflectance in the final paint.

1. Introduction

Buildings are responsible for more than 40 percent of global energy use and one third of global greenhouse gas (GHG) emissions. This fact has made energy efficiency and savings strategies a priority for energy policies at world level [1,2].

Especially important has been the intensification of energy consumption in Heating, ventilation and air conditioning (HVAC) systems accounting for around 40% of total building consumption [3,4] and being the largest energy end use both in the residential and non-residential sector.

The EPBD (European Directive o the Energy Performance of Buildings) [5] was adopted with the objective of "promote the improvement of the energy performance of buildings within the community taking into account outdoor climatic and local conditions, as well as indoor climate requirements and cost-effectiveness". Building sector has the greatest potential to deliver quick, deep and cost effective reductions in GHG emissions [6,7].

The majority of the building stock in Europe is pre-1990 and 40–50% is pre-1960. In order to address the huge challenge of affordable building refurbishment, different solutions are being explored with the aim of obtaining substantial energy savings at an acceptable investment [8,9].

Solutions from the chemical and materials science can bring significant energy savings for building applications being the *high reflectance outdoor coatings* one of the most promising ones [10]. These coatings reflect sunlight radiation in the infrared part of the spectrum. Since nearly half of the solar radiation consists of near-infrared (NIR) radiation (700–2500 nm) which is a direct consequence of heat, the use of NIR reflective materials aids to preserve lower exterior surface temperatures of buildings [11,12]. The amount of heat conducted to the interior decreases being possible to save up to 15% of air conditioning energy consumption depending on the climate region. Costs of applying these coatings are affordable and offer reasonable payback times [10].

These high reflectance coatings mainly refer to paints containing cool pigments. Although white pigments such as titanium dioxide (TiO_2) have a high solar reflectance, they cannot always satisfy the consumer's demand as they are white. One strategy for non-white cool pigment production is the use of complex inorganic colored pigments (CICPs). One barrier for the use of these pigments is their

* Corresponding authors.
E-mail addresses: estibaliz.aranzabe@tekniker.es (E. Aranzabe), maribel.arriortua@ehu.es (M.I. Arriortua).

http://dx.doi.org/10.1016/j.enbuild.2016.05.011
0378-7788/

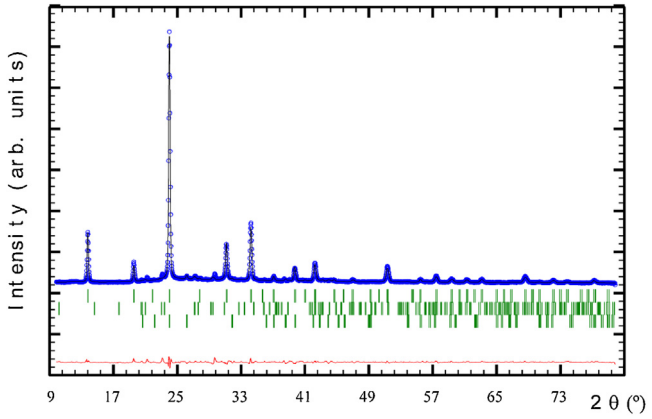

Fig. 1. X-ray diffraction refinement for the Ultramarine pigment. Circles denote experimental points; upper solid line is calculated profile. Theoretical peak positions (vertical sticks) and difference line are shown in the bottom of the pattern.

toxicity character as most of them contain toxic metal elements (Co, Cd, Pb, Cr) restricted by the environmental regulations [13,14].

Ultramarine blue pigment (UB) is an inorganic pigment having a sodium aluminum silicate sulfide structure ($Na_8Al_6Si_6O_{24}S_2$) similar to Sodalite. Ultramarine blue are a family of low-cost mineral pigments (cost 3–5 times lower than a CICP) and with high pigmentary properties commonly used in construction sector.

The aim of this study is to develop a cool pigment based on ultramarine blue. The strategy to modify this conventional pigment into a high reflecting pigment is to coat the pigment with a coating containing nanoparticles with a crystal structure of rutile or corundum (structures used for the CICP development).

Dispersed nanoparticles in the pigment coating will provoke multiple scattering effects achieving high reflection between 700 and 2500 nm. The suitable nanoparticles and the amount of particles in the coating are one of the most important parameter that must be optimized to achieve the fixed goal. Alumina (having a size of 13 nm) and titania (having a size of 21 nm) nanoparticles were selected due to their high diffraction index and strong light scattering.

2. Experimental part

2.1. Materials

2.1.1. Ultramarine pigment

A standard ultramarine blue pigment produced by Nubiola Pigmentos S.L. was used. Ultramarine pigment compositions are based on the crystal chemistry of the royal blue Sodalite mineral Lazurite [$Na_6Ca_2Al_6Si_6O_{24}(S_n,SO_4)_2$].

The particle size distribution of the pigment was analyzed using a Malvern Mastersizer 2000 at the same conditions explained above. A stable and mono-modal distribution was obtained for this system being the main particle size d_{50} of 1.2 μm.

The scanning electron microscope (SEM) micrograph indicates rather irregular shape of the pigment particles with a particle size in the range from 1 μm to 2 μm in good agreement with the particle size distribution results.

The purity of the sample was evaluated by standard X-Ray diffraction measurements. The identification of the pattern was evaluated, in all the cases, using the Powder Diffraction File (PDF) database. PANalytical XíPert High Score program was used for identification and Miller indexing of all the observed maxima. Moreover, the selected patterns used for the identification of the

Table 1
Processed pigments (nanoparticle type and concentration added to the titania coating).

Pigment	Added nanoparticles to the coating solution	%wt. nanoparticles[a]
Pigment 1	Al_2O_3	2
Pigment 2		4
Pigment 3		6
Pigment 4		8
Pigment 5	TiO_2	2
Pigment 6		4
Pigment 7		6
Pigment 8		8
Pigment 9	50%	2
Pigment 10	Al_2O_3 + 50%TiO_2	4
Pigment 11		6
Pigment 12		8

[a] related to the coating solution weight.

Table 2
DL and TSR of processed pigment.

Alumina (Al_2O_3)			
Pigment	%wt. Pig	TSR (%)	DL
1	5	62.95	72.57
(2 wt%)	10	55.72	61.04
	15	51.87	53.59
2	5	63.08	73.35
(4 wt%)	10	56.87	61.44
	15	51.58	53.84
3	5	66.69	73.74
(6 wt%)	10	56.8	61.62
	15	51.64	54.54
4	5	66.43	74.26
(8 wt%)	10	55.72	62.42
	15	51.81	54.22
Titania (TiO_2)			
Pigment	%wt. Pig	TSR (%)	DL
5	5	62.41	71.86
(2 wt%)	10	56.15	62
	15	51.88	54.97
6	5	64.9	72.37
(4 wt%)	10	56.47	61.44
	15	49.95	52.14
7	5	65.73	73.28
(6 wt%)	10	56.51	60.85
	15	51.7	53.68
8	5	66.22	72.57
(8 wt%)	10	55.4	61.96
	15	52.82	55.14
Mixture (50%Alumina + 50%Titania)			
Pigment	%wt. Pig	TSR (%)	DL
9	5	64.45	72.55
(2 wt%)	10	55.95	60.44
	15	52.03	54.36
10	5	66.27	73.39
(4 wt%)	10	56.01	61.22
	15	52.36	54.49
11	5	66.27	73.16
(6 wt%)	10	58.15	62.44
	15	51.81	55.11
12	5	65.45	73.96
(8 wt%)	10	56.6	61.97
	15	52.89	55.26
Reference (un-modified blue)			
Pigment	%wt. Pig	TSR (%)	DL
Original	0	80.98	94.61
	5	58.26	64.54
	10	53.86	58.94
	15	51.26	57.03

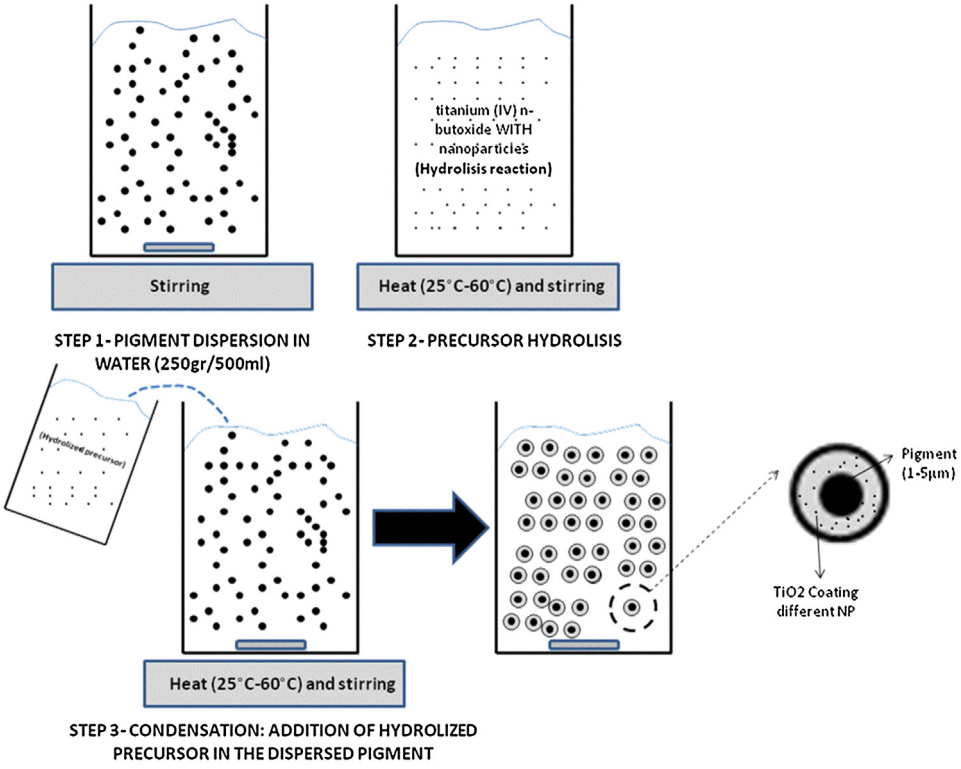

Fig. 2. Pigment coating process description.

observed phases, were refined using the full-profile refinement without structural model by FullProf [15,16].

The obtained results were in good agreement with Sodalite "Sodium Aluminum Silicate Chlorate "(01-082-1811) and small impurities of Nepheline "Sodium Potassium Aluminum Silicate" (01-071-0954) and Aluminum Phosphate (01-084-0854) (see Fig. 1).

The observed impurities and their semi quantitative analysis obtained from the refinement are ~10% and ~1% in weight for Nepheline and Aluminum Phosphate, respectively.

The experimental and calculated data agreed being the final reliability factor: s Rp: 6.27, Rwp: 8.83, Chi2: 5.36 and Bragg R-factor: 0.58 for the Sodalite.

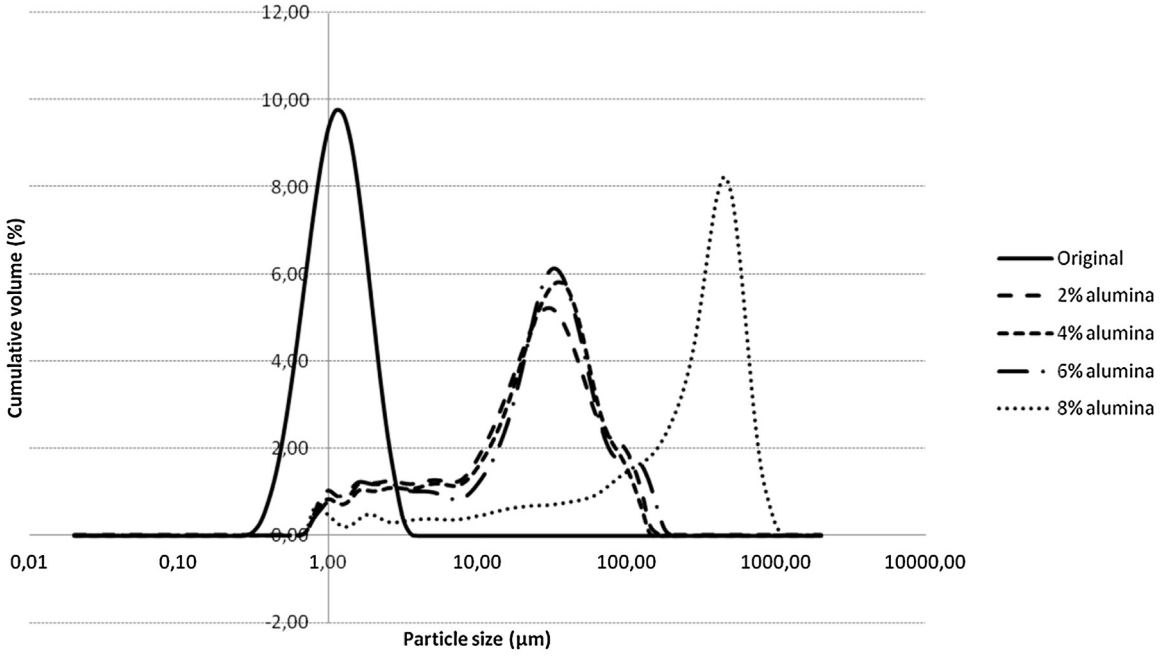

Fig. 3. Particle size distribution of the original pigment and pigments coated with a coating having a titania matrix containing Al_2O_3 nanoparticles at different percentages.

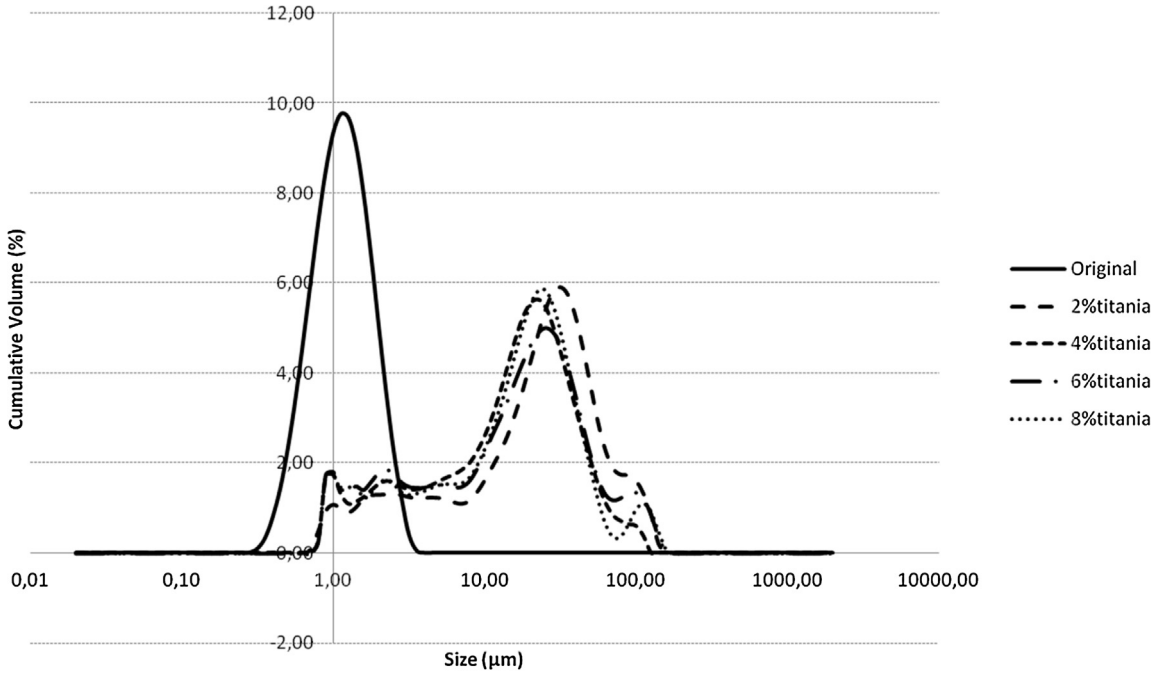

Fig. 4. Particle size distribution of the original pigment and pigments coated with a TiO2 coating containing TiO2 nanoparticles at different percentages.

2.1.2. Nanoparticles

Commercial alumina nanoparticles in powder form with a primary particle size of 13 nm and a surface area of 85–115 m^2/g were purchased from Sigma-Aldrich.

Commercial titania nanoparticles (consisting of 71% anatase and 27% rutile) in powder form with a primary size of 21 nm and a surface area of 35–65 m^2/g were purchased from Sigma-Aldrich.

XRD preliminary identification of the initial phases evaluated using the Powder Diffraction File (PDF) were in agreement with Aluminum Oxide (00-029-0063) and anatase ~80% (01-073-1764)/rutile ~20% (01-087-0710).

The deconvolution of the non overlapped more intense diffraction maxima using the peak-fit option of the WinPLOTR program without structural model was used to calculate the broadening of the diffraction signal. The average coherently diffracting domains of the samples were extracted from the broadening of the signal using the Scherrer equation:

$$\beta_{hkl} = k \times \lambda / L_{hkl} \times \cos\theta$$

where β_{hkl} is the broadening of the diffraction line measured at half the line maximum intensity (FWHM) taking in to account instrumental contribution ($\beta_{Inst} = 0.1^\circ$), λ is the X-ray wavelength, L_{hkl} is the crystal size and θ is the diffraction angle. K is the Scherrer shape factor (K = 0.9 was used for the calculations). The calculated crystallite sizes are near 10, 25 and 30 nm for alumina, anatase and rutile, respectively.

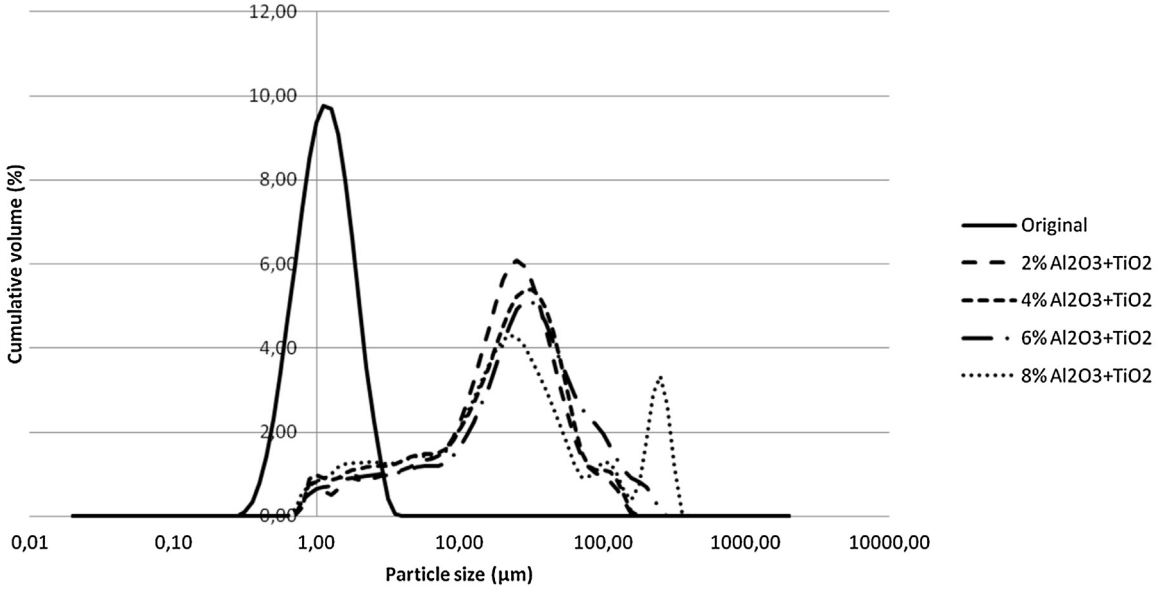

Fig. 5. Particle size distribution of the original pigment and pigments coated with a TiO_2 coating having $TiO_2 + Al_2O_3$ nanoparticles at different percentages.

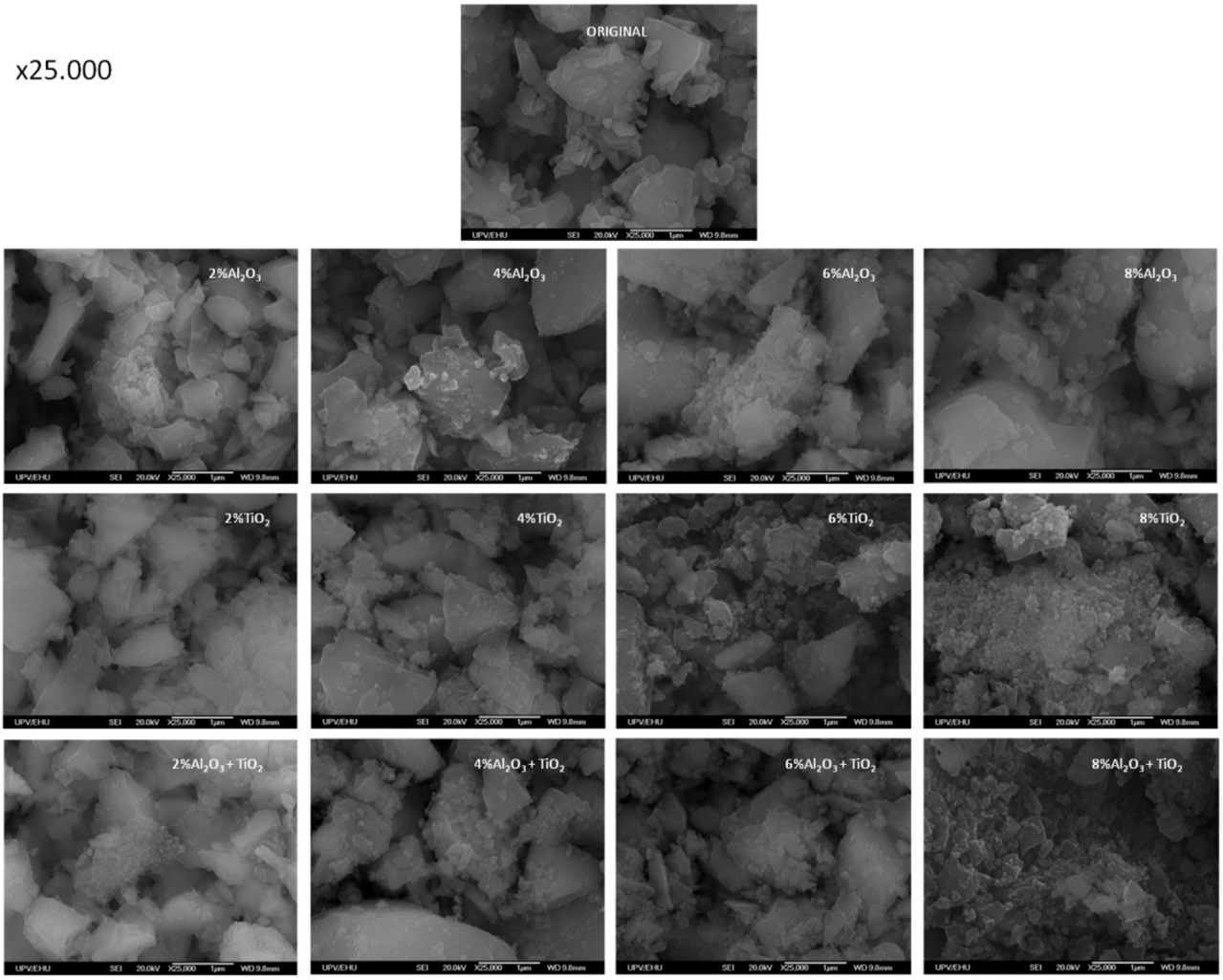

Fig. 6. Scaning electron micrographs of the raw and modified ultramarine blue pigments.

2.2. Instrumental methods

The crystal structures of the compounds were studied by powder *X-Ray Diffraction (XRD)* technique. The measurements were collected in a PHILIPS X'PERT PRO automatic diffractometer in theta–theta configuration. Secondary monochromator with Cu-Kα radiation (λ = 1.5418 Å) (40 kV 40 mA) and a PIXcel solid state detector (active length in 2θ 3.347°) was used. XRD data were collected from 10 to 80° 2θ each 0.026° and 500 s at RT. Zero background silicon wafer and fixed divergence and antiscattering slit giving a constant volume of sample illumination were used.

The *Scanning Electron Microscopy (SEM)* micrographs were recorded with Hitachi S-4800 equipment using Secondary Electron Detector at 3 kV accelerating voltage and 8 mm working distance.

The particle size distribution (0.02–2000 μm range) of the samples was analyzed using *Laser Dispersion* by Malvern Mastersizer 2000 after keeping the sample in ultrasonic agitation for 2 min. Water was used as the dispersion media and a particle Refractive Index of 1.510 was considered for the measurement and 5 cycles of measurement were done.

Concerning the reflection capability of the pigments in the Near Infrared, two parameters (Total Solar Reflectance and Lightness) were measured in a paint containing different percentages of pigments.

Total Solar Reflectance (TSR) is the percentage of irradiated energy that is reflected by an object. The total solar reflectance calculation requires taking the raw reflectance data and applying solar weighting factors for each wavelength collected. TSR of the obtained samples was measured according to ASTM G173 in a Perkin Elmer Lambda 950 UV/Vis/NIR System in the wavelength range from 300 to 2500 nm.

The TSR of two materials can be compared only if their tinting strength (DL) is the same, so was decided to establish the relation between DL (lightness) and TSR for each material as the lightness (CIELAB lightness L *) is related to the tinting strength. DL was measured in a Perkin Elmer Lambda 950 UV/Vis/NIR System in the wavelength from 380 nm to 780 nm.

3. Results

3.1. Modification of the ultramarine pigment with the aim of improving its reflecting capability in the NIR

Reflecting films based on a TiO_2 matrix containing different types and concentration of nanoparticles (alumina, titania and a mixture of them) were deposited around the reference pigment surface. For this issue, the pigment was put in dispersion in water at 50 g/l. Separately a solution of titanium (IV) *n*-butoxide containing different types and concentration of nanoparticles was hydrolyzed and added drop by drop to the pigment dispersion (see Fig. 2) obtaining a coated pigment. The coating around the pigment sur-

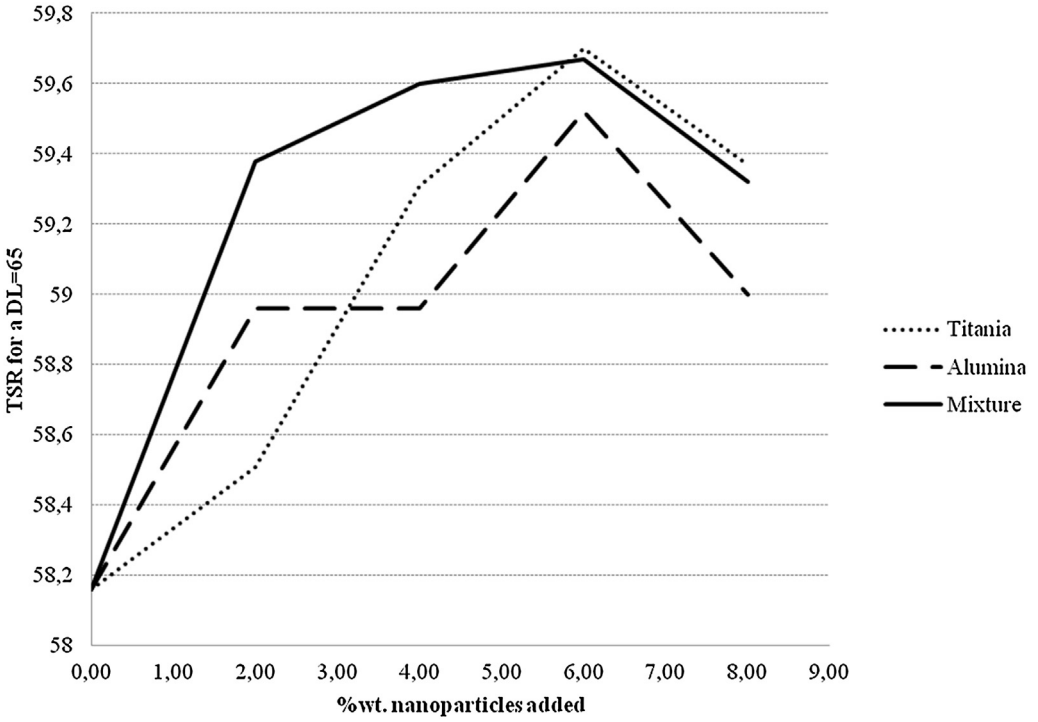

Fig. 7. Total Solar Reflectance of paints containing different percentages of nanoparticles (for a DL = 65).

face was based on a titanium dioxide matrix containing different types of nanoparticles (alumina, titania and a mixture of them).

The maximum concentration of nanoparticles added to the solution was 8% wt. related to the coating solution weight as for higher concentrations the nanoparticles tended to sedimentation.

Once the solution was added, obtained pigments were filtered and cured at 150 °C during 12. Table 1 summarizes the prepared samples and the conditions associated to these experiments.

With the aim of evaluating the improvements of the processes pigments, they were characterized in terms of:

→ Particle size distribution (in order to measure the dispersability of the processed pigments)

→ Total Solar Reflectance (TSR) of the processes pigments for a standard DL = 65 corresponding to an appropriate lightness value when applied to conventional paints.

3.1.1. Laser diffraction

The particle size distribution of the obtained pigments was analyzed using a Malvern Mastersizer 2000 at the same conditions explained above. Fig. 3 shows the results obtained for pigment having the TiO_2 matrix coating containing Al_2O_3 nanoparticles at different percentages

Particle size of pigments particles in paint is a critical parameter affecting surface finish, tinting strength but also rheological characteristics. A stable and mono-modal distribution was obtained for the original system with a mean particle size of 1.2 μm. It was decided not to use pigments with a mean particle size of 50 μm for paint application as it could affect strongly to the rheology of the paint.

Agglomerates with a mean size around 20 μm was obtained for pigments additivated with 2, 4 and 6 wt% of alumina nanoparticles. An increase in the amount of nanoparticles led to higher agglomeration being the mean particle size of 350 μm.

In the case of the pigment having the TiO_2 matrix coating containing TiO_2 nanoparticles at different percentages, a mean size around 30 μm was obtained for pigments additivated with 2, 4, 6 and 8 wt% of titania nanoparticles (see Fig. 4).

Table 3
TSR of processed pigments for a DL = 65.

Percentage of NP	Titania	Alumina	Mixture
0	58.16		
2%	58.51	58.96	59.38
4%	59.31	58.96	59.60
6%	**59.70**	**59.52**	**59.67**
8%	59.37	59.00	59.32

The particle size distribution of the pigment having the TiO_2 matrix coating containing 50wt%TiO_2 + 50wt%Al_2O_3 nanoparticles at different percentages is shown in Fig. 4. A mean size around 30 μm was obtained for pigments additivated with 2, 4 and 6 wt% of nanoparticles. An increase in the amount of nanoparticles leds to a bimodal distribution obtaining some agglomerates with a mean particle size of 110 μm.

Pigments containing more than 6 wt% of alumina tend to agglomerates higher than 50 μm being an obstacle to obtain good dispersions in paints. Pigments containing more than 6 wt% of the mixture of alumina and titania presents a bimodal distribution leading to a non-stable dispersion which can cause some dispersability problems (Fig. 5).

3.1.2. - scanning electronic microscopy (SEM)

Fig. 6 shows the scanning electron microscope (SEM) micrographs of the processed samples. Some agglomerates appear in samples containing 8%wt. of nanoparticles in good agreement with previous laser dispersion measurements.

3.2. Paint additivation with the modified pigments with the aim of improving its reflecting capability in the NIR

An interior water-based paint was selected as the matrix to disperse the pigments at different percentages. For the paints preparation, 5, 15 and 25 wt% of pigments were mechanically dis-

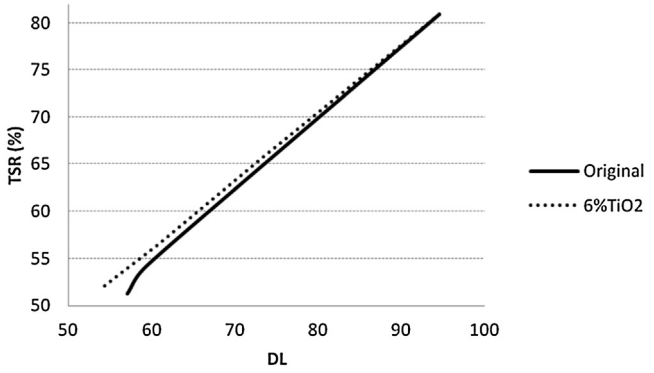

Fig. 8. Total Solar Reflectance vs DL of the paint containing 6% of titania nanoparticles compared to the reference.

persed with the base paint. Stainless steel substrates were painted with a layer of 50 μm of thickness.

3.2.1. - NIR-UV-vis spectroscopy

The reflection capability in the Near Infrared, the Total Solar Reflectance and Lightness were measured in the final paints.

Table below shows the materials prepared and the obtained values for DL and TSR (Tables 2).

For each pigment, the linear equation relating TSR and DL was calculated. Once, the equation is defined, the TSR for a standard DL value of 65 was calculated obtaining the values shown in Table 3. This lightness value graduation of 65 can be considered a conventional value for the paint application.

All the obtained pigments increased the TSR of the original pigment when adding nanoparticles. Maximum values in all the cases were obtained for additions of 6%wt. of nanoparticles (see Fig. 7 - results for 6%wt. in bold). High agglomeration of nanoparticles (agglomerates higher than 100 μm) detected by laser dispersion led to less reflectance in the final paint.

The mixture of titania and alumina nanoparticles provides higher TSR for all the added concentrations excluding the case of 6 wt.% where the TSR for titania nanoparticles and the mixture of titania and alumina provided a similar TSR.

The nanoparticle providing the higher TSR is titania in a 6%wt. TSR trend vs DL can be seen in Fig. 8.

4. Conclusions

In this study, a ultramarine blue pigment has been coated with different reflecting films based on TiO_2 and containing different types and concentration of nanoparticles (alumina, titania and a mixture of them). These pigments have been dispersed in a conventional waterborne paint at different percentages to be evaluated.

As Total solar Reflectance depends strongly on color and tinting strength, the linear equation relating DL (lightness) and TSR for each material has been calculated and the TSR has been compared for a standard DL value of 65.

All the obtained pigments increased the TSR of the original pigment when adding nanoparticles but the maximum value was obtained for an addition of 6%wt. of titania nanoparticles. Agglomeration of nanoparticles detected by laser dispersion led to less reflectance in the final paint.

Acknowledgements

This project has received founding from the European Union Seventh Framework Programme (FP7-NMP-2010-Small-5) under grant agreement no. 280393 and from the Dpto. Educación, Política Lingüística y Cultura of the Basque Goverment (IT-630-13), Ministerio de Ciencia e Innovación (MAT2013-42092-R) and Engineering and Physical Sciences Research Council (EP/I003932). SGIker technical support (UPV/EHU, MEC, GV/EJ, European Social Fund) is gratefully acknowledged.

References

[1] Transition to Sustainable Buildings Strategies and Opportunities to 2050, International Energy Agency (IEA), 2012, ISBN 978-92-64-20241-2.
[2] C. Li, T. Hong, D. Yan, Appl. Energ. 131 (2014) 394–410.
[3] P. Nejat, F. Jomehzadeh, M. Mahdi Taheri, M. Gohari, M.Z. Majid, Renew. Sustain. Energy Rev. 43 (2015) 843–862.
[4] L. Perez-Lombard, J. Ortiz, C. Pout, Energy Build. 40 (3) (2008) 394–398.
[5] Directive 2010/31/EU of the European Parliament and of the Council of 19 May 2010 on the energy performance of buildings Official Journal of the European Union, L153/13 (2010).
[6] D. D'Agostino, J. Build. Eng. 1 (2015) 20–32.
[7] Common carbon metric for Measuring Energy Use & Reporting Greenhouse Gas Emissions from Building Operations Sustainable Buildings and Climate Initiative (2010).
[8] F. Zhao, et al., Reconstructing building stock to replicate energy consumption data, Energy Build. (2015), http://dx.doi.org/10.1016/j.enbuild.2015.10.001.
[9] R. Ruparathna, K. Hewage, R. Sadiq, Renew. Sustain. Energy Rev. 53 (2016) 1032–1045.
[10] Innovative Chemistry for Energy Efficiency of Buildings in Smart Cities L. Bax, J., Cruxent, J., Komornicki, European Technology Platform for Sustainable Chemistry and SmartCities and Communities (2013).
[11] X. Zhao, Y. Zhang, Y. Huang, H. Gong, J. Zhao, Dyes Pigm. 116 (2015) 119–123.
[12] J.A. Prakash, S. Laha, S. Natarajan, M.L. Reddy, Dyes Pigm. 107 (2014) 118–126.
[13] H.R. Hedayati, A.A. Sabbagh Alvani, H. Sameie, R. Salimi, S. Moosakhani, F. Tabatabaee, A. Amiri Zarandi, Dyes Pigm. 113 (2015) 588–595.
[14] A. Han, M. Ye, L. Liu, W. Feng, M. Zhao, Energy Build. 84 (2014) 698–703.
[15] H.M. Rietveld, A profile refinement method for nuclear and magnetic structures, J. Appl. Cryst. 2 (1969) 65–71.
[16] J. Rodríguez-Carvajal, Recent advances in magnetic structure determination by neutron powder diffraction, Phys. B Condens. Matter 192 (1993) 55–69.